⌘ *Author's Choice*

THE JOURNAL OF BIOLOGICAL CHEMISTRY VOL. 288, NO. 12, pp. 8531–8543, March 22, 2013


# Characterization of a Cdc42 Protein Inhibitor and Its Use as a Molecular Probe*[S]

Received for publication, November 12, 2012, and in revised form, January 17, 2013 Published, JBC Papers in Press, February 4, 2013, DOI 10.1074/jbc.M112.435941

**Lin Hong[‡§], S. Ray Kenney[¶], Genevieve K. Phillips[‖], Denise Simpson[**], Chad E. Schroeder[**], Julica Nöth[**], Elsa Romero[‡], Scarlett Swanson[‡], Anna Waller[‡§], J. Jacob Strouse[‡§], Mark Carter[‡§], Alexandre Chigaev[‡], Oleg Ursu[§‖‡‡], Tudor Oprea[§‖‡‡], Brian Hjelle[‡], Jennifer E. Golden[**], Jeffrey Aubé[**§§], Laurie G. Hudson[¶‖], Tione Buranda[‡], Larry A. Sklar[‡§‖1,2], and Angela Wandinger-Ness[‡¶1,3]**

*From the [‡]Department of Pathology, [§]University of New Mexico (UNM) Center for Molecular Discovery, [¶]Department of Pharmaceutical Sciences, [‖]Cancer Research and Treatment Center, and [‡‡]Department of Biochemistry and Molecular Biology, University of New Mexico, Albuquerque, New Mexico 87131, the [**]University of Kansas Specialized Chemistry Center, Lawrence, Kansas 66047, and the [§§]Department of Medicinal Chemistry, University of Kansas, Lawrence, Kansas 66045*

**Background:** By integrating extracellular signals with actin cytoskeletal changes, Cdc42 plays important roles in cell physiology and has been implicated in human diseases.
**Results:** A small molecule was found to selectively inhibit Cdc42 in biochemical and cellular assays.
**Conclusion:** The identified compound is a highly Cdc42-selective inhibitor.
**Significance:** The described first-in-class Cdc42 GTPase-selective inhibitor will have applications in drug discovery and fundamental research.

**Cdc42 plays important roles in cytoskeleton organization, cell cycle progression, signal transduction, and vesicle trafficking. Overactive Cdc42 has been implicated in the pathology of cancers, immune diseases, and neuronal disorders. Therefore, Cdc42 inhibitors would be useful in probing molecular pathways and could have therapeutic potential. Previous inhibitors have lacked selectivity and trended toward toxicity. We report here the characterization of a Cdc42-selective guanine nucleotide binding lead inhibitor that was identified by high throughput screening. A second active analog was identified via structure-activity relationship studies. The compounds demonstrated excellent selectivity with no inhibition toward Rho and Rac in the same GTPase family. Biochemical characterization showed that the compounds act as noncompetitive allosteric inhibitors. When tested in cellular assays, the lead compound inhibited Cdc42-related filopodia formation and cell migration. The lead compound was also used to clarify the involvement of Cdc42 in the Sin Nombre virus internalization and the signaling pathway of integrin VLA-4. Together, these data present the characterization of a novel Cdc42-selective allosteric inhibitor and a related analog, the use of which will facilitate drug development targeting Cdc42-related diseases and molecular pathway studies that involve GTPases.**

The Ras-related GTPase superfamily contains ~150 members of small monomeric guanine nucleotide binding proteins. This superfamily is further divided into subfamilies based on sequence as well as functional similarities. Cdc42 is a member of the Rho GTPase subfamily and was first identified in *Saccharomyces cerevisiae* as a mediator of cell division (1). Since then, Cdc42 has been found to be well conserved in organisms ranging from yeast to mammals (2). As a GTPase, Cdc42 functions in a binary mode with the GTP-bound state active and the GDP-bound state inactive. Three classes of proteins regulate the activity status of Cdc42. Guanine nucleotide exchange factors (GEFs)[4] facilitate GDP dissociation and GTP binding and thus convert Cdc42 to the active state; GTPase-activating proteins catalyze the hydrolysis of bound GTP and return Cdc42 to the inactive state (3); and guanine nucleotide dissociation inhibitors (GDIs) sequester Cdc42 in the inactive GDP-bound state (4). The GTP-bound Cdc42 can interact with multiple downstream effectors and activate a range of molecular pathways. For its functions in cytoskeleton organization, the GTP-bound Cdc42 binds and activates the kinase p21-activated protein kinase, which then phosphorylates and activates LIM kinase, a zinc finger domain-containing protein. This initiates actin polymerization, which is important for establishing adherens junctions, invasion, and migration (5). The activated p21-activated protein kinase is also known to phosphorylate Raf1

* This work was supported by National Science Foundation (NSF) Grant MCB0956027 and National Institutes of Health Grant R03 MH081231-01 from the Molecular Libraries Program (to A. W. N.); University of New Mexico Center for Molecular Discovery Molecular Libraries Probe Production Centers (UNMCMD MLPCN) National Institutes of Health Grants U54MH084690 and R01HL081062 (to L. A. S.); UNM National Center for Research Resources (NCRR) Grant 5P20RR016480 (to L. G. H.); National Institutes of Health Grant R21 CA170375-01 through the NCI (to A. W. N., L. G. H., and J. E. G.); National Institutes of Health Grants NS066429 and AI092130 (to T. B.); and University of Kansas Specialized Chemistry Center (KUSCC) MLPCN National Institutes of Health Grant U54HG005031 (to J. A.).
⌘ *Author's Choice*—Final version full access.
[S] This article contains supplemental Equations 1–3, supplemental text, and Figs. S1–S3.
[1] These two authors should be regarded as co-senior authors.
[2] To whom correspondence may be addressed. E-mail: lsklar@salud.unm.edu.
[3] To whom correspondence may be addressed. E-mail: wness@unm.edu.

[4] The abbreviations used are: GEF, guanine nucleotide exchange factor; GDI, guanine nucleotide dissociation inhibitor; MTS, 3-(4,5-dimethylthiazol-2-yl)-2,5-diphenyltetrazolium bromide; fMLFF, formyl-Met-Leu-Phe-Phe; FAM, 6-carboxyfluorescein; TAMRA, 6-carboxytetramethylrhodamine; LDV, 4-((*N*′-2-methylphenyl)ureido)-phenylacetyl-L-leucyl-L-aspartyl-L-valyl-L-prolyl-L-alanyl-L-alanyl-L-lysine; ANOVA, analysis of variance; DMSO, dimethyl sulfoxide; VLA-4, very late antigen-4.

and MEK to enhance the signal through ERK and thus help to define the transcription profiles of multiple downstream genes (6). The aberrant activation of these genes frequently leads to oncogenic transformation. For its role in vesicle trafficking, Cdc42 has been shown to recruit the Par complex to the apical membrane to facilitate the exocytosis of vesicles that contain the apical markers (7). It also acts in combination with various factors such as PI3K, neuronal Wiskott-Aldrich syndrome protein (N-WASP), and transducer of Cdc42-dependent actin assembly Toca-1) to regulate membrane tubulation in endocytosis (8).

Considering its diverse functions, it is not surprising that malfunctions of Cdc42, its upstream regulators, and it downstream effectors have been associated with many diseases. Higher expression levels of Cdc42 are known to correlate with increased testicular cancer progression and poorer outcome (9). Overexpression of Cdc42 has also been found in lung cancer and cutaneous melanoma and may serve as a disease marker and prognosis parameter (10–12). Moreover, the Cdc42 downstream effector Par was shown to be expressed at high levels in prostate cancer and radiation-treated medulloblastoma (13). BetaPix, a Cdc42 GEF, is overexpressed in human breast cancer (14), whereas in ovarian cancer, the activity of Cdc42 was found to be amplified by upstream signal transducers (15–17). Therefore, inhibiting Cdc42 could be a useful approach in both cell biology studies and disease treatment.

The currently available inhibitors of Cdc42 include *Clostridium difficile* toxin B (18) and secramine (19), both of which are limited in their uses. *C. difficile* toxin B inhibits Cdc42 by adding a glucose moiety to a serine residue through post-translational modification, blocking the association of Cdc42 with membranes and preventing downstream signal transduction. This mechanism of action is similar to some Ras GTPase inhibitors, which also act by impeding the interaction of Ras and the plasma membrane (20). As for secramine, it stabilizes the interaction of Cdc42 and RhoGDI1 and thus locks Cdc42 in an inactive state. In terms of selectivity of these agents, *C. difficile* toxin B modifies not only Cdc42 but also Rho and Rac, whereas the RhoGDIs that can be sequestered by secramine are also regulators for Rho and Rac. Restricting RhoGDIs in a complex with Cdc42 by secramine could affect the activation status of Rho and Rac. Therefore, these inhibitors lack specificity and as such, may induce off-target-associated toxicity and possess limited utility in selective interrogation of Cdc42 involvement in complex cellular pathways. The compound we report here was identified by high throughput screening of the Molecular Libraries Small Molecule Repository (21–23). From about 200,000 compounds, 398 were found to decrease fluorescent GTP binding to one or more GTPases at 10 $\mu$M. Among them, CID29950007 was chosen for its novel selectivity profile. To the best of our knowledge, the compound is the first Cdc42 nucleotide binding inhibitor ever reported (23). Here it is characterized both mechanistically and in cellular assays to show its utility as a molecular probe.

## EXPERIMENTAL PROCEDURES

*Materials*—GST-tagged GTPases were either from Cytoskeleton or purified as described previously (24). Cyto-Plex™ microspheres (4.0 $\mu$m) were from Thermo Fisher Scientific. BODIPY® FL GTP and BODIPY® FL GDP were from Life Technologies. LDV (4-((*N*′-2-methylphenyl)ureido)-phenylacetyl-L-leucyl-L-aspartyl-L-valyl-L-prolyl-L-alanyl-L-alanyl-L-lysine) and its FITC-conjugated analog (LDV-FITC) were synthesized by Commonwealth Biotechnology as described previously (25). *N*-Formyl-Met-Leu-Phe-Phe (fMLFF) was purchased from Sigma-Aldrich. MTS was from Promega, and phenazine methosulfate was from Pierce. DAPI and Boyden chambers were from Thermo Scientific. Reagents were otherwise from Sigma-Aldrich if not specified. Swiss 3T3 cells and Vero E6 cells were from ATCC. OVCA429 and SKOV3ip cells were acquired through a material transfer agreement with MD Anderson Cancer Center. OVCA429 cells were cultured in Eagle's minimal essential medium (26), and SKOV3ip cells were cultured in RPMI 1640 medium (26). The cell cultures were passaged according to the provided protocols. Sin Nombre virus strain S77734 was propagated according to the protocol approved by the biosafety committee of the University of New Mexico (Public Health Service Registration Number C20041018-0267). The HyperCyt® delivery system and the CyAn™ ADP flow instrument were from IntelliCyt® and Beckman Coulter, respectively.

*Synthetic Preparation, Purification, and Analytical Characterization of CID2950007 and CID-44216842*—Experimental details are given in the supplemental data.

*Dose-response Inhibition by CID2950007 and Its Analog CID44216842*—The assay was carried out according to our previously described protocols (21, 23). Briefly, each individual GST-tagged enzyme was incubated with glutathione-coated microsphere beads overnight with gentle rotation. The microsphere beads were labeled with a red fluorescent dye at varying intensities and therefore could be separated by a flow cytometer. The unbound GTPases were removed by sufficient washing. The bead sets were then combined. Compound CID2950007 or CID44216842 at different concentrations and BODIPY® FL GTP were then added. Final concentrations of the compounds ranged from 100 $\mu$M to 15 nM. The mixtures were incubated at 4 °C for 2 h with gentle rotation. The beads were sipped and delivered with the HyperCyt® instrument and read on a CyAn™ ADP flow cytometer. Forward scatter and side scatter were used to define the whole bead population. FL9 channel (excitation/emission: 635/750LP nm) was used to separate different bead sets. FL1 channel (excitation/emission: 488/530 nm) measures the FITC fluorescence associated with the beads. As a separate control, GST-tagged GFP was bound to a set of glutathione beads to which CID2950007 or CID44216842 was added to ensure that any fluorescence changes observed in the assay reaction were not due to fluorescence quenching, but due to the *bona fide* inhibition of fluorescent nucleotide binding.

*Association and Dissociation Time Course*—Fluorescence measurements were made with a spectrofluorometer (Photon Technology International). The excitation and emission wavelengths were 480 and 530 nm, respectively. BODIPY® FL GTP at 500 nM in a HEPES buffer (30 mM HEPES, pH 7.2, 40 mM KCl, 100 mM NaCl, 0.1% (v/v) Nonidet P-40, 1 mM DTT, 1 mM EDTA and 0.1% BSA) was first added to a 7 × 45-mm glass cuvette

(Sienco) followed by an equal amount of buffer containing either 400 nM enzyme or 400 nM enzyme plus 10 μM compound. The fluorescence changes were immediately recorded. For the dissociation kinetic studies, either compound at a final concentration of 10 μM or GTP at 250 μM was added to the reaction. The dissociation time course was fitted to a single exponential equation (supplemental Equation 1) to obtain $k_{off}$. The concentration of GTP or CID2950007 did not affect the determination of the dissociation rate constant.

*Equilibrium Binding Assay*—Wild-type GST-Cdc42 was bound to GSH beads in NP-HPSE buffer (30 mM HEPES, pH 7.2, 40 mM KCl, 100 mM NaCl, 1 mM EDTA and 0.1% (v/v) Nonidet P-40) overnight at 4 °C. The beads were washed twice and resuspended with NP-HPSE buffer supplemented with 0.1% BSA and 1 mM DTT. CID2950007 at a final concentration of 10 μM and increasing concentrations of BODIPY® FL GTP were added to the suspension. Samples were incubated at 4 °C for 2.5 h, and binding of the fluorescent nucleotide to the enzyme was measured using the CyAn™ ADP flow cytometer. Raw data were exported, and the curves were fitted using the one-site binding equation (supplemental Equation 2) from GraphPad Prism 5.

*Cytotoxicity Assays*—Cells were cultured in growth medium and tested using either MTS or CellTiter-Glo (Promega) assays. For OVCA429 and SKOV3ip, cells were plated in 12-well plates at $1 \times 10^4$ cells/well and allowed to attach for 4 h. Then, fresh medium containing CID2950007 ranging from 0.1 to 10 μM was added to replace the old medium. The cells were allowed to grow for 95 h before being treated with 600 μM MTS reagents and 25 μM phenazine methosulfate for 2 h. Reactions were stopped by the addition of 10% sodium dodecyl sulfate. Absorbance at 490 nm was read using a SpectraMax microplate reader (Molecular Devices). For U937 ΔST, Swiss 3T3, and Vero E6 cells, the CellTiter-Glo luminescent cell viability assay was conveniently conducted according to manufacturer's protocol. Briefly, cells were seeded in 96-well plates. Compounds were tested at increasing concentrations (0.5–30 μM) for 1–48 h in accordance with the doses and times employed in the cellular assays using these cell lines. After adding luciferase substrate, the luminescence was read on a plate reader. Seeding cell densities were confirmed to be in the linear range of the luminescence change.

*GLISA*—Swiss 3T3 cells were continuously passaged at subconfluence and used to monitor the capacity of compounds to block stimulus-mediated activation of Cdc42 or Rac1 *in vivo*. Vero E6 cells are responsive to calpeptin-mediated stimulation of RhoA and thus were used as a second cell line for assessing compound effects on RhoA activity. Commercial GLISA kits customized to capture activated Cdc42, Rac1, or RhoA from cell lysates were used per manufacturer's instructions (Cytoskeleton). Cells were serum-starved by sequentially removing serum over a 3-day period and treated with either 0.1% DMSO or 1 or 10 μM compound for 60 min. Subsequently, samples were treated with 100 ng/ml EGF for 2 min to activate Cdc42 or Rac1 or with 1 μg/ml calpeptin for 30 min to activate RhoA. DMSO-treated cells were left either unstimulated to determine base-line GTPase activation or stimulated without drug treatment to determine maximal GTPase activation. Cell lysates were frozen, and active Cdc42 and Rac1 were quantified based on a p21-activated protein kinase binding assay (27), whereas active RhoA was quantified based on a rhotekin binding assay (28). All assays were performed in 96-well microtiter plates. Purified GTP-loaded Cdc42, Rac1, or RhoA control proteins were included in each assay to quantify active GTPases in the lysates.

RhoA activation was independently confirmed by monitoring actin stress fiber formation following calpeptin stimulation (1 μg/ml) for 30 min. Actin filaments in control and stimulated cells were detected following paraformaldehyde (4%) fixation and Triton X-100 (0.5%) permeabilization using Alexa Fluor® 488 phalloidin (1 unit, or ~0.17 μM) (Life Technologies).

*Immunofluorescence Staining and Microscopy*—Filopodia formation was measured according to established protocols (29). Briefly, Swiss 3T3 cells were grown on coverslips. Bradykinin at 100 ng/ml was added to stimulate cells for 10 min. Cells were washed with phosphate-buffered saline and fixed with 4% paraformaldehyde followed by permeabilization for 5 min with 0.1% Triton X-100 in Tyrode's buffer and blocking for 1 h with 1% BSA in Tyrode's buffer. Cells were stained with rhodamine phalloidin to label filamentous actin and then mounted in ProLong® Gold (Life Technologies). A Zeiss LSM510 META with 63 × 1.4 NA objective was used to acquire the images at 1024 × 1024 pixels. To study the compound effect, cells were treated with CID2950007 (10 μM, from 10 mM stock in DMSO) or DMSO (0.1%, v/v) for 1 h before the addition of bradykinin. CID44216842 was similarly tested in one trial (10 μM, from 10 mM stock in DMSO). Trends were similar to those shown for CID2950007 without reaching statistical significance and therefore are not shown. For each condition, 30–60 cells were randomly chosen and imaged. Filopodia were defined as hair-like protrusions, positive for actin 0.5–1 μm in diameter. The number and length of filopodia present on each cell were measured using SlideBook software. SlideBook traces of filopodia measured in pixels were converted to μm based on 1 μm = 28 pixels for 63× image at 1024 × 1024 pixels. The experiment was repeated three times.

*Cell Migration Assay*—OVCA429 and SKOV3ip cells were plated at $1 \times 10^4$ cells/well in 24-well Boyden chambers and allowed to attach for 4 h. Then, compounds at final concentrations ranging from 0.1 to 10 μM were added to the growth media. After 48 h, inserts were removed and stained with DAPI. Membrane filters were imaged on a Zeiss inverted microscope using a 20× objective, and three representative fields were counted from each treatment group.

*Host-Virus Interaction Assay*—For infection assays, Vero E6 cells were incubated with 10 μM CID2950007 for 30–45 min before being exposed to infectious Sin Nombre virions (multiplicity of infection ~0.1) for 30 min in the presence of compound. Control cells were treated with 0.1% DMSO in lieu of compound. Following virus entry, unbound Sin Nombre virions were removed with low pH buffer treatment for 1 min and washed three more times in PBS. The low pH buffer contained 40 mM sodium citrate, pH 3.0, 10 mM KCl, and 135 mM NaCl. The cells were then incubated in medium either with or without the compound for 24 or 48 h. TaqMan RT-PCR was used to measure viral S-segment 24–48 h after infection according to

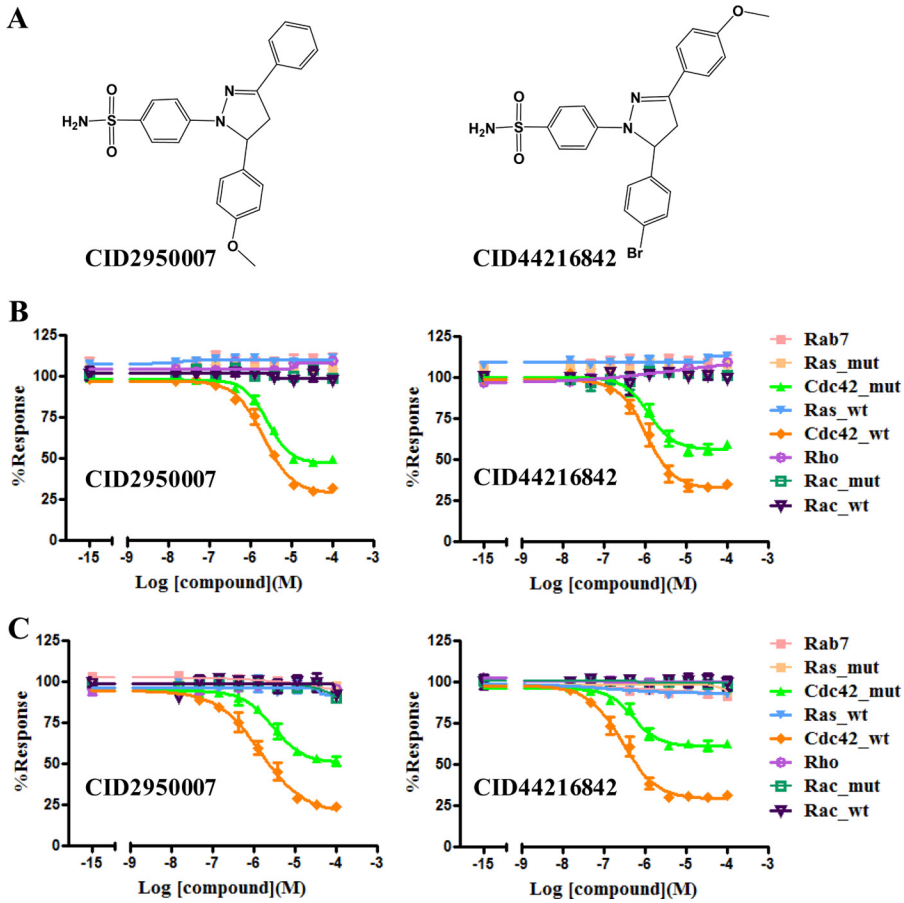


FIGURE 1. **Two structural analogs selectively inhibit Cdc42 nucleotide binding activity.** *A*, structures of CID2950007 and its analog CID44216842. *B*, the concentration effects of CID2950007 and CID44216842 on eight GTPases. The curves were fitted to the sigmoidal dose-response equation using GraphPad Prism. The percentage of response was calculated as the ratio of (sample MCF − negative control MCF)/(positive control MCF − negative control MCF) (where MCF is median channel fluorescence). For the positive control, DMSO instead of the compound was added; for the negative control, the compound was replaced with GTP at a concentration 5000-fold greater than BODIPY® FL GTP. The $EC_{50}$ for Cdc42 wild type and Cdc42Q61L mutant were 2.1 and 2.6 $\mu$M, respectively, for CID2950007 and 1.0 and 1.2 $\mu$M, respectively, for CID44216842. *C*, the concentration effects of the two compounds on BODIPY® FL GDP binding to eight GTPases. The $EC_{50}$ values for Cdc42 wild type and Cdc42Q61L mutant were 1.4 and 2.9 $\mu$M, respectively, for CID2950007 and 0.3 and 0.5 $\mu$M, respectively, for CID44216842. Data shown are representative of at least three independent sets of measurements with each set conducted in duplicate.

previously described procedures (30, 31). Briefly, viral RNA was extracted from cells using the RNeasy kit and reverse-transcribed with SuperScript III (Life Technologies). The primer was an S-segment-specific sense primer (5′-agcacattacagagcagacgggc-3′). The resulting DNA was PCR-amplified with S-segment-specific primers (5′-gcagacgggcagctgtg-3′ and 5′-agatcagccagttcccgct-3′) and a fluorescently labeled TaqMan probe (5′-FAM-tgcattggagaccaaactcggagaactt-TAMRA-3′) in triplicate reactions using Taq Gold. The fluorescence was measured on an ABI Prism 7000 sequence detection system (Life Technologies). A standard curve drawn from S-segment template of known copy numbers was used to quantify the viral RNA.

*LDV Binding Assay*—The procedure was based on an established protocol with minor changes (25, 32). The U937 FPRΔST cell, which has desensitizing mutations toward *N*-formyl peptide (33), was used to extend the signal observation window. The cells were grown in RPMI 1640 supplemented with 2 mM L-glutamine, 100 units/ml penicillin, 100 $\mu$g/ml streptomycin, and 10% heat-inactivated fetal bovine serum. For the binding experiment, cells at $0.4-0.8 \times 10^6$ cells/ml were constantly stirred with a magnetic stir bar, and the fluorescence was recorded on a FACScan flow cytometer (Block Scientific). LDV-FITC at a final concentration of 4 nM and *N*-formyl peptide at 100 nM were sequentially added followed by the addition of either compound at different concentrations or an equal volume of DMSO. Nonfluorescent LDV was added at 1 $\mu$M to dissociate the remaining LDV-FITC. The inhibition percentage was calculated according to supplemental Equation 3. The experiment has been repeated at least three times.

*Statistical Analyses*—One-way ANOVA with Dunnett's post test was conducted to compare differences between the means of each group relative to the control group for cytotoxicity, migration, GLISA, filopodia, virus infection, and integrin activation assays. Statistical significance was accepted at $p < 0.05$ and denoted by an *asterisk* in the figures. GraphPad Prism was used to perform statistical analyses.

## RESULTS

*CID2950007 and Its Analog Specifically Inhibit GTP Binding to Cdc42*—Compound CID2950007 and its analog CID44216842 were synthesized as described in the supplemental data. The effect of each compound on the binding of BODIPY® FL GTP to eight different GTPases was comparatively assessed in a multiplex assay (Fig. 1). The eight GTPases

are H-Ras and its G12V constitutively active mutant; Cdc42 and its Q61L constitutively active mutant; Rac1 and its Q61L constitutively active mutant; and RhoA and Rab7, which are representative members of the Ras, Rho, and Rab subfamily GTPases. The compounds inhibited BODIPY® FL GTP binding to both Cdc42 and its mutant in a dose-dependent manner. The inhibition was specific toward Cdc42 with no effects on other GTPases including Rac and Rho in the same family (Fig. 1*B*). Compound CID44216842 had a slightly improved $EC_{50}$ as compared with CID2950007 for both Cdc42 and its mutant. However, biophysical characterization showed that the analog had decreased solubility. Therefore, CID2950007 remained the primary focus of subsequent characterizations. The fluorescence decrease was confirmed to be due to *bona fide* inhibition of BODIPY® FL GTP binding and not a result of fluorescence quenching (see "Experimental Procedures," data not shown). The nucleotide identity appears not to be essential for the inhibition by CID2950007 because the compound also selectively inhibited BODIPY® FL GDP binding to Cdc42 and its mutant (Fig. 1*C*). The concentration of the fluorescent guanine nucleotide in the assay was fixed close to its $K_d$. According to the Cheng-Prusoff equation (34), the $EC_{50}$ obtained under our assay condition is a close estimate of the $K_i$ of the compound. Residual fluorescent GTP binding was observed even at high compound concentrations. Remaining activity may suggest the presence of multiple conformers of the commercially obtained Cdc42 protein and its mutant. To the best of our knowledge, CID2950007 and its analog are the first small molecules that show specific inhibition of nucleotide binding toward Cdc42 GTPase.

*CID2950007 Is a Noncompetitive Inhibitor*—To examine the mechanism of CID2950007 inhibition, its effects on the equilibrium binding and the binding and dissociation kinetics of BODIPY®-labeled guanine nucleotide were assessed. The fluorescence of BODIPY®-labeled guanine nucleotide will increase when bound to GTPases due to release of steric hindrance (35, 36). The change can be captured in real time on a fluorometer. First, the nucleotide content of the enzymes used was quantified, and it was found that the GST-tagged enzymes were mostly apo-proteins (supplemental data). Then, the inhibition mechanism was studied in a kinetic dissociation assay. When Cdc42 was added to a solution of BODIPY® FL GTP, there was a fluorescence increase indicating the binding of the nucleotide to the protein. After equilibrium was reached, either GTP or CID2950007 was added. The dissociation of BODIPY®-labeled nucleotide was observed, but with different kinetics in the two cases (Fig. 2*A*). When the time course was fitted to a single exponential equation, the calculated dissociation rate constants were 0.008 and 0.002 $s^{-1}$, respectively. Therefore, GTP and CID2950007 induced the dissociation of BODIPY®-labeled guanine nucleotide through different mechanisms. Although GTP directly competed with the fluorescent nucleotide by binding to the active site of Cdc42, CID2950007 likely provoked the dissociation by binding to a location other than the active site. In the subsequent equilibrium binding assay, the binding of BODIPY® FL GTP to Cdc42 was measured in the presence or absence of 10 $\mu$M CID2950007 (Fig. 2*B*). The binding curves were fitted to a hyperbolic one-site binding equation (supplemental Equation 2). Both the maximum fluorescence ($B_{max}$), which is indicative of the maximum guanine nucleotide binding that can be achieved, and the apparent dissociation constant $K_d$ changed (Fig. 2*B*). A competitive inhibitor will be outcompeted by BODIPY® FL GTP of high concentrations. Therefore, the $B_{max}$ will remain the same in the presence of a competitive inhibitor. The observed significant change on $B_{max}$ suggests a noncompetitive mechanism of action from CID2950007. Moreover, in the kinetic binding studies, before being added to the solution of BODIPY® FL GTP, the enzyme Cdc42 was either not treated or added with compound CID2950007 (Fig. 2*C*). If the compound can bind to Cdc42 as a fast binding competitive inhibitor (34), we should expect to see BODIPY® FL GTP bind to the inhibited Cdc42 at a different rate as compared with binding to the uninhibited Cdc42. Also, the fluorescent level that could be achieved from BODIPY® FL GTP binding should be much lower. These expectations were contrary to observation. In the presence of the inhibitor, BODIPY® FL GTP bound to Cdc42 at a rate comparable with that in the absence of the inhibitor and achieved a comparable fluorescence level, arguing against a competitive mechanism. A fluorescence decrease, which is a reflection of BODIPY® FL GTP departure, was only observed after a significant fluorescence increase, suggesting that CID2950007 binds to an allosteric site of Cdc42 only after the enzyme has been loaded with BODIPY® FL GTP at the active site and then induces the dissociation of the nucleotide. An analogous binding curve was observed when CID2950007 was replaced with its analog CID44216842, confirming the lack of artifacts associated with CID2950007 (Fig. 2*D*, *blue curve*). EDTA in the buffer facilitated nucleotide binding and association and allowed the kinetics to be studied in a tractable time frame. Without EDTA, CID2950007 still induced BODIPY® FL GTP dissociation from Cdc42, although at a slower rate (Fig. 2*E*). In these kinetic studies, the hydrolysis of BODIPY® FL GTP was not resolved, possibly due to the low intrinsic hydrolysis activity of GTPases (37). However, it was found that the identity of the guanine nucleotide was not important. CID2950007 similarly induced the dissociation of BODIPY® FL GDP (Fig. 2*F*) where hydrolysis was not an issue. This observation corroborates the result that CID2950007 inhibited BODIPY® FL GDP binding in a dose-dependent manner with comparable $EC_{50}$ values (Fig. 1). Finally, the effect of CID2950007 is specific toward Cdc42 with no activity toward Ras and Rac1 (Fig. 2, *G* and *H*). Together, these findings are consistent with the notion that CID2950007 is a selective noncompetitive and most likely conformation-dependent allosteric inhibitor that binds to guanine nucleotide-bound Cdc42, induces the dissociation of the ligand, and locks the protein in an inactive conformation (Fig. 2*I*).

*Cell-based Analyses of CID2950007 Demonstrate in Vivo Utility for Identifying and Characterizing Cdc42-dependent Processes*—Cdc42 is important for actin remodeling, endocytosis, cell adhesion, and migration. Therefore, the identified Cdc42 inhibitor was tested in a variety of cell-based assays to demonstrate utility for cellular analyses of Cdc42 functions. Processes well known to depend on Cdc42 (filopodia formation and cell migration) were used first to establish cellular activity, and subsequently, the effect of the inhibitor was tested in situ-

ations where Cdc42 activity was implicated (hantavirus entry and integrin activation), but not yet directly demonstrated.

*Assessment of Cytotoxicity*—The cytotoxicity of compounds CID2950007 and CID44216842 was assessed in cells including neutrophils, fibroblasts, kidney epithelia, and ovarian cancer lines based on either formazan dye or luminescence assays. OVCA429 and SKOV3ip cell lines are both from human ovary carcinomas where Cdc42 is activated by upstream signal transducers (15–17). CID2950007 was not cytotoxic in either cell line at doses of 0.1–3 $\mu$M after treatment for 4 days (Fig. 3, *A* and *B*). OVCA429 cells were insensitive to 10 $\mu$M compound, whereas some cytotoxicity was observed in SKOV3ip cells at this concentration after a 4-day treatment, although it did not reach statistical significance. CID2950007 was not cytotoxic

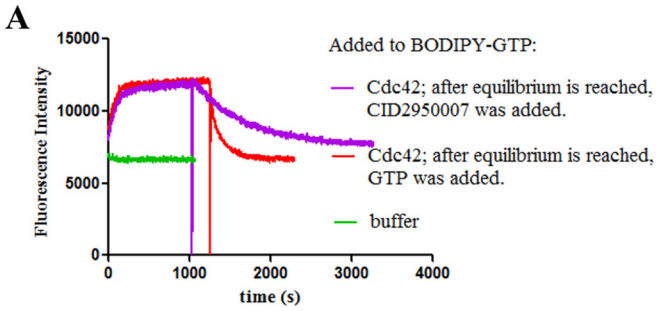


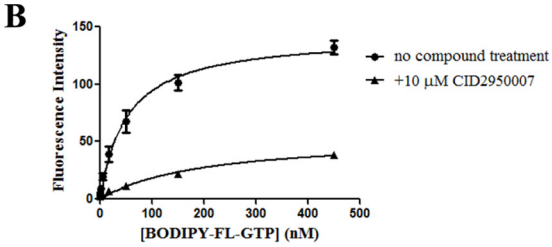


| One site-Specific binding | no compound treatment | + 10 μM CID2950007 |
|---|---|---|
| Bmax | 142.5 | 54.21 |
| Kd (nM) | 50.8 | 195.7 |

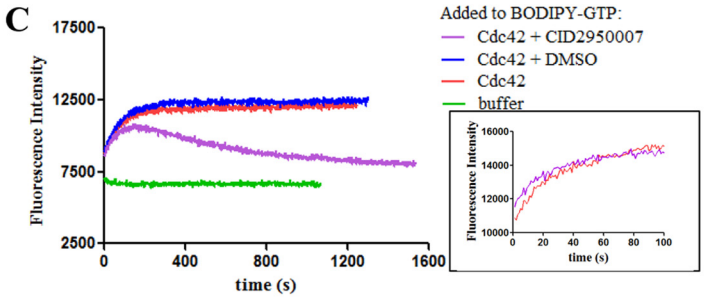


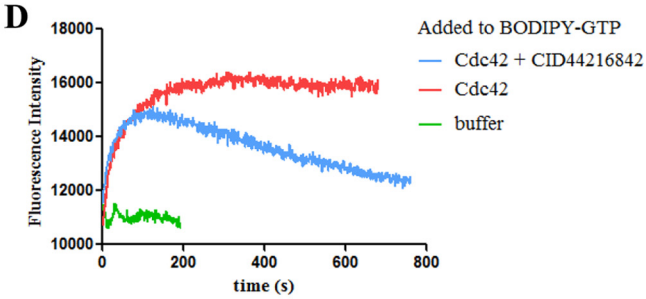


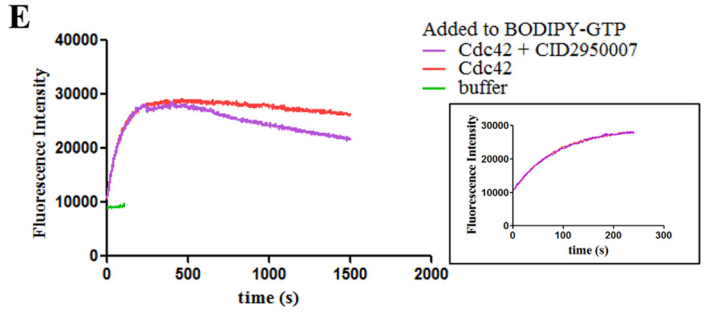


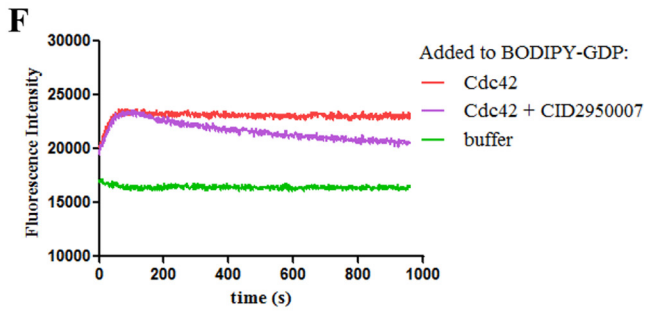


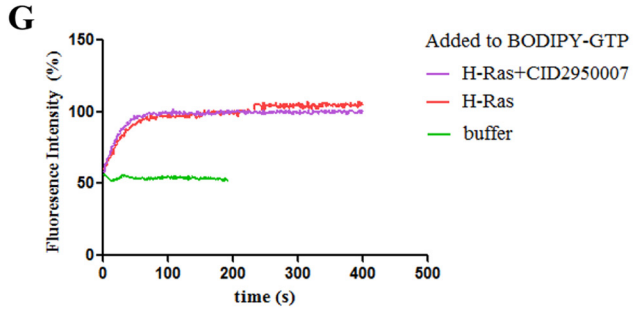


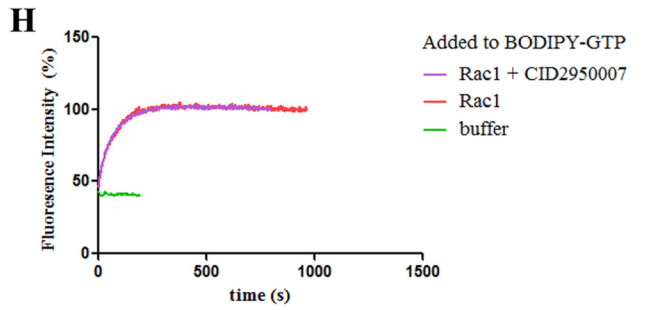


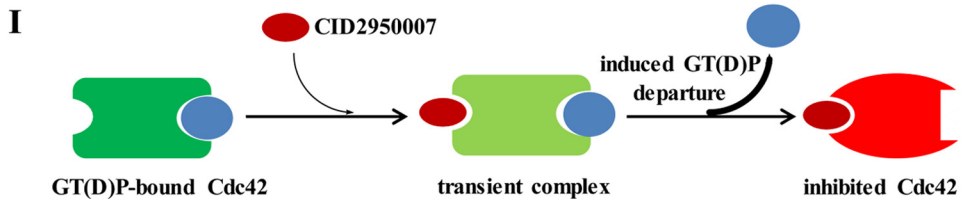

toward Swiss 3T3 or Vero E6 cells up to 10 μM for 24 and 48 h, respectively (Fig. 3, *C* and *D*). Neither CID2950007 nor CID44216842 was cytotoxic toward U937ΔST cells at concentrations up to 10 μM for 24 h and up to 30 μM after 1 h (Fig. 3, *E–H*). All subsequent cell-based assays were performed using CID2950007 or CID44216842 at concentrations and incubation times where no cytotoxicity was evident.

*CID2950007 and CID44216842 Inhibit Stimulus-induced Cdc42 Activation, but Not Rac1 and RhoA*—Effector protein binding assays (GLISA) were used to assess the ability of the compounds to inhibit Cdc42 activation in cells and monitor its selectivity relative to other Rho family members. Swiss 3T3 fibroblasts were treated with each of the compounds and then subjected to EGF stimulations to activate Cdc42 and Rac1. Compound effects on RhoA activation were measured in Vero E6 kidney epithelia cells after calpeptin stimulation. Both compounds significantly inhibited Cdc42 activation at 10 μM, whereas neither compound inhibited Rac1 or RhoA activation at the same concentration (Fig. 4, *A–C*). The GLISA data are consistent with *in vitro* blockade of the interaction between Cdc42 and p21-activated protein kinase measured using a biochemical pull-down assay (21). Thus, the compounds exhibit Cdc42 selectivity in cell-based assays and can be used to assess Cdc42 dependence of cellular pathways and processes.

*CID2950007 Inhibits 3T3 Fibroblast Filopodia Formation*—Filopodia are Cdc42-induced cytoplasmic projections containing bundled actin filaments with functions in cell adhesion, migration, and invasion (29, 38). Filopodia formation is enhanced by chemotropic cues, enabling cell migration along a directed path. As expected, stimulation of 3T3 fibroblasts by bradykinin treatment increased both the numbers and the length of filopodia formed on the expanding edge relative to resting control cells (Fig. 5*A*). However, when the cells were incubated with 10 μM CID2950007 for 1 h prior to bradykinin treatment, both the number and the average length of filopodia were decreased (Fig. 5, *B* and *C*). DMSO (0.1%, v/v) treatment as a control had no effect on filopodia formation relative to bradykinin stimulation, but did increase filopodia length similar to bradykinin, most likely due to the cell ruffling effect of DMSO that has been previously reported (39, 40). Because CID2950007 must be dissolved in DMSO and diluted into aqueous solution, the inhibitory effect of the compound is demonstrated by its ability to counteract the stimulatory effects of both DMSO and the bradykinin cue. Together, the data demonstrate that CID2950007 is a potent inhibitor of filopodia formation, a process that is well known to be directly regulated by Cdc42.

*CID2950007 Inhibits Ovarian Cancer Cell Migration*—Cdc42-induced filopodia are important to the mobility of many cell types (41, 42). Down-regulation of Cdc42 through genetic methods reduces the ability of cells to manage directed migration in a chemokine gradient (43). Ovarian cancer is characteristically metastatic, and Cdc42, which is activated by p70 S6 kinase in ovarian cancer, has been speculated to be accountable for the migratory phenotype (16). In a Boyden chamber assay, CID2950007 clearly inhibited the migration of human ovarian carcinoma cell lines OVCA429 and SKOV3ip in a dose-dependent manner (Fig. 6, *A* and *B*). At 3 μM, the compound reduced cell migration to less than 50% of the untreated control. Importantly, there was no cytotoxicity for either OVCA429 or SKOV3ip at this concentration (Fig. 3, *A* and *B*). In addition, a commercially available Rac inhibitor NSC23766 also completely inhibited OVCA429 migration at 10 μM (data not shown). Cdc42 and Rac1 are known to be involved in cell migration through distinct pathways (44, 45). However, the coordinate function and the relative importance of each pathway have been incompletely assessed, and previous studies have largely relied on mutant GTPase overexpression. The fact that inhibition of either GTPase alone with small molecule inhibitors could restrain migration indicates an important interplay between Rac- and Cdc42-regulated pathways in ovarian cancer cell migration.

*CID2950007 Inhibits Cdc42-regulated Virus Infection*—Due to its roles in actin cytoskeleton organization and vesicle trafficking, Cdc42 is frequently involved in the pathogen internalization during viral infections (8). Cdc42 may regulate the formation of macropinosomes; however, its exact roles in viral infection are not well understood. Previous studies have largely depended on the use of Cdc42-activating and -inactivating mutants or broad spectrum Rho inhibitors such as *C. difficile* toxin B (46–48). Only recently has secramine been used to inhibit the cell-to-cell spread of HIV (49). Sin Nombre virus causes hemorrhagic fever that is associated with significant mortality and morbidity. The mechanistic details regarding its uptake are unknown. To test the potential role played by Cdc42 and its effectors, host cells were incubated with CID2950007 and infected with Sin Nombre virus. The amount of the viral RNA was quantified 24–48 h later. CID2950007 treatment only during the initial virus exposure gives an estimation of Cdc42 requirement for virus entry, whereas compound treatment for 24–48 h demonstrates nearly complete inhibition of viral replication (Fig. 7). Therefore, the use of CID2950007 establishes for the first time a role for Cdc42 in Sin Nombre virus internalization. The results further suggest that the inhi-

FIGURE 2. **CID2950007 is an allosteric inhibitor of Cdc42.** *A*, compound CID2950007 and GTP induce the dissociation of BODIPY® FL GTP through different mechanisms. After BODIPY® FL GTP bound to Cdc42, either 250 μM GTP (*red*) or 10 μM CID2950007 (*purple*) was added. The fluorescence curves were fitted to a single exponential equation to get dissociation rate constants (supplemental Equation 1). The concentration of GTP or CID2950007 did not affect the determination of the dissociation rate constant. *B*, the presence of CID2950007 changed both $B_{max}$ and $K_d$ in the BODIPY® FL GTP equilibrium binding assay. *C*, CID2950007 inhibited BODIPY® FL GTP binding. An equal amount of buffer (*green*), 400 nM Cdc42 (*red*), 400 nM Cdc42 + 0.1% DMSO (*blue*), or 400 nM Cdc42 + 10 μM CID2950007 (*purple*) was added to a solution of 500 nM BODIPY® FL GTP. The *inset* shows the expanded view of the initial fluorescence change. *D*, analog CID44216842 has similar effects as CID 2950007 toward BODIPY® FL GTP binding to Cdc42. *E*, buffer was the same as that in *A* except that without EDTA, CID2950007 inhibited BODIPY® FL GTP binding at a slower rate. The *inset* shows the expanded view of the initial fluorescence change. *F*, CID2950007 inhibits BODIPY-GDP binding to Cdc42 similar to BODIPY-GTP binding. *G* and *H*, CID2950007 did not inhibit BODIPY® FL GTP binding to Ras (*G*) or Rac1 (*H*). Fluorescence intensity was normalized as percentage using the equilibrium reading as the maximum against which the percentage was obtained. Conditions were the same as that in *A*. *I*, model of the CID2950007 inhibition mechanism. After guanine nucleotide binds to Cdc42, CID2950007 associates with the complex and induces the dissociation of the guanine nucleotide. The resulting Cdc42 complex is locked in an inactive conformation. Experiments were performed in at least duplicates. Representative curves are shown.

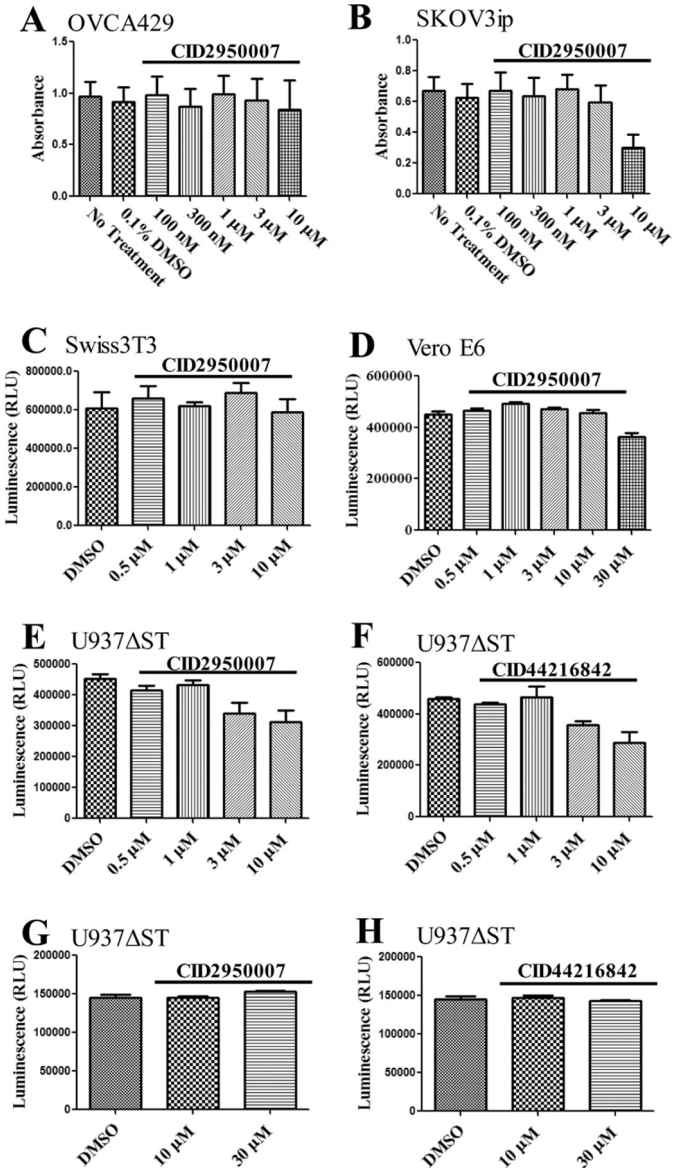


FIGURE 3. **CID2950007 did not show cytotoxicity in multiple cell lines.** *A* and *B*, cell viability measured toward OVCA429 (*A*) and SKOV3ip (*B*) cells after a 4-day incubation at 0.1–10 $\mu$M using MTS assay. *C–H*, cell viability measured using luminescence assay. *C*, compound CID2950007 tested on Swiss 3T3 cells at concentrations of 0.5–10 $\mu$M for 24 h. *D*, compound CID2950007 tested on Vero E6 cells at concentrations of 0.5–10 $\mu$M for 48 h. *E* and *F*, compound CID2950007 tested on U937 ΔST cells up to 10 $\mu$M for 24 h (*E*) and up to 30 $\mu$M for 1 h (*F*). *G* and *H*, compound CID44216842 tested on U937 ΔST cells up to 10 $\mu$M for 24 h (*G*) and up to 30 $\mu$M for 1 h (*H*). *A* and *B* represent three independent trials with assays conducted in duplicate or triplicate. From *C–H*, experiments were conducted in at least triplicate. Means ± S.E. from all trials are plotted. For compound treatments at the experimental concentrations and time durations, there were no differences with $p < 0.05$ based on one-way ANOVA with Dunnett's post test and relative to either untreated control cells (*A* and *B*) or DMSO-treated cells (*C–H*). Statistical significance assessment was the same using either as the comparison group. *RLU*, relative light units.

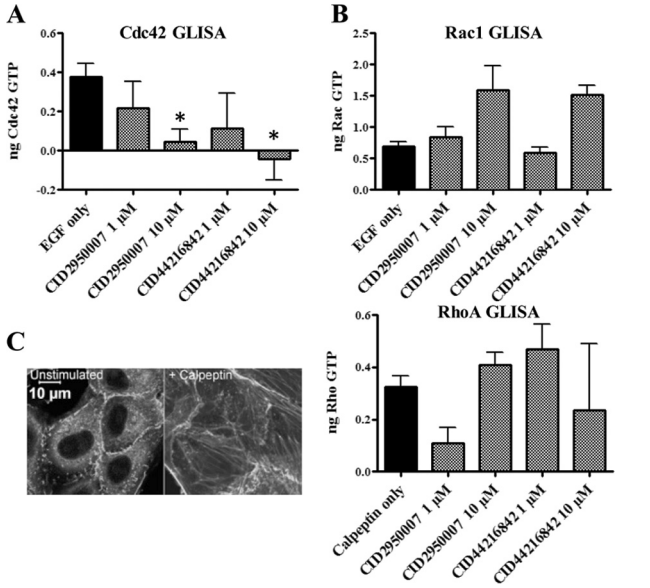


FIGURE 4. **Cdc42 activation was specifically inhibited by CID2950007 and its analog CID44216842 as demonstrated by the GLISA assay.** *A* and *B*, Swiss 3T3 cells were serum-starved and then pretreated with compounds CID2950007 or CID44216842 at indicated concentrations as detailed under "Experimental Procedures." Cells were subsequently stimulated with EGF to activate Cdc42 or Rac1 and compared with unstimulated cells. Control cells were mock-treated with 0.1% DMSO to account for compound diluent. After cell lysis, the amounts of active Cdc42 or Rac1 were quantified based on p21-activated protein kinase binding by GLISA. The following conditions were used: Cdc42, nine independent trials for CID2950007 and two independent trials for CID44216842 with duplicate or triplicate samples for each condition; Rac1, three independent trials for CID2950007 with duplicate or triplicate samples and one trial for CID44216842 with triplicate samples. *C*, Vero E6 cells were serum-starved, treated with CID2950007 or CID44216842, and stimulated with calpeptin to activate RhoA with one trial in triplicate. Immunofluorescence micrograph confirms RhoA activated stress fiber formation. Purified GTP-loaded Cdc42, Rac1, or RhoA control proteins were used to calculate the ng of activated GTPase. Means ± S.E. with EGF control subtracted from all trials are plotted. *Asterisks* denote $p < 0.05$ based on one-way ANOVA with Dunnett's post test and relative to EGF- or calpeptin-stimulated control cells.

bition of Cdc42 by CID2950007 will be useful for more broadly testing the requirement for Cdc42 in the entry of other viruses.

*CID2950007 Inhibits LDV Binding to VLA-4 Integrin*—Very late antigen-4 (VLA-4) is an integrin commonly expressed on the leukocyte plasma membrane. At the site of injury, the chemotactic agent released by the infecting object stimulates the conformational change of VLA-4, which can then bind with high affinity to the integrin receptor vascular cell adhesion molecule-1 (VCAM-1) that is expressed on the endothelium. The arrest of the leukocyte subsequently initiates a cascade of immune responses. Strong evidence supports the involvement of Rho and Rac GTPases in the signaling pathway that is activated by chemotactic ligands and leads to integrin conformational change (50–52). Whether Cdc42, which is in the same GTPase family, also plays a role has not been previously clarified. A real-time flow cytometry-based assay was used to demonstrate the usefulness of CID2950007 in this cellular context. A fluorescently labeled LDV peptide, LDV-FITC, was used in which the LDV peptide constitutes the fragment of VCAM-1 that interacts with VLA-4. The activation status of VLA-4 could be monitored by the fluorescence associated with the VLA-4-expressing U937 cells. The cells initially bound LDV-FITC at the basal level. After fMLFF stimulation, VLA-4 changed to a high affinity state, which was accompanied by increased LDV-FITC binding. The fluorescence level of the cells was therefore increased. The addition of CID2950007 and its analog caused a dose-dependent loss of fluorescence due to reduced VLA-4 affinity and LDV dissociation, whereas the same amount of DMSO had no effect (Fig. 8). The inhibition is faster than that observed in the biochemical kinetic binding assay, possibly

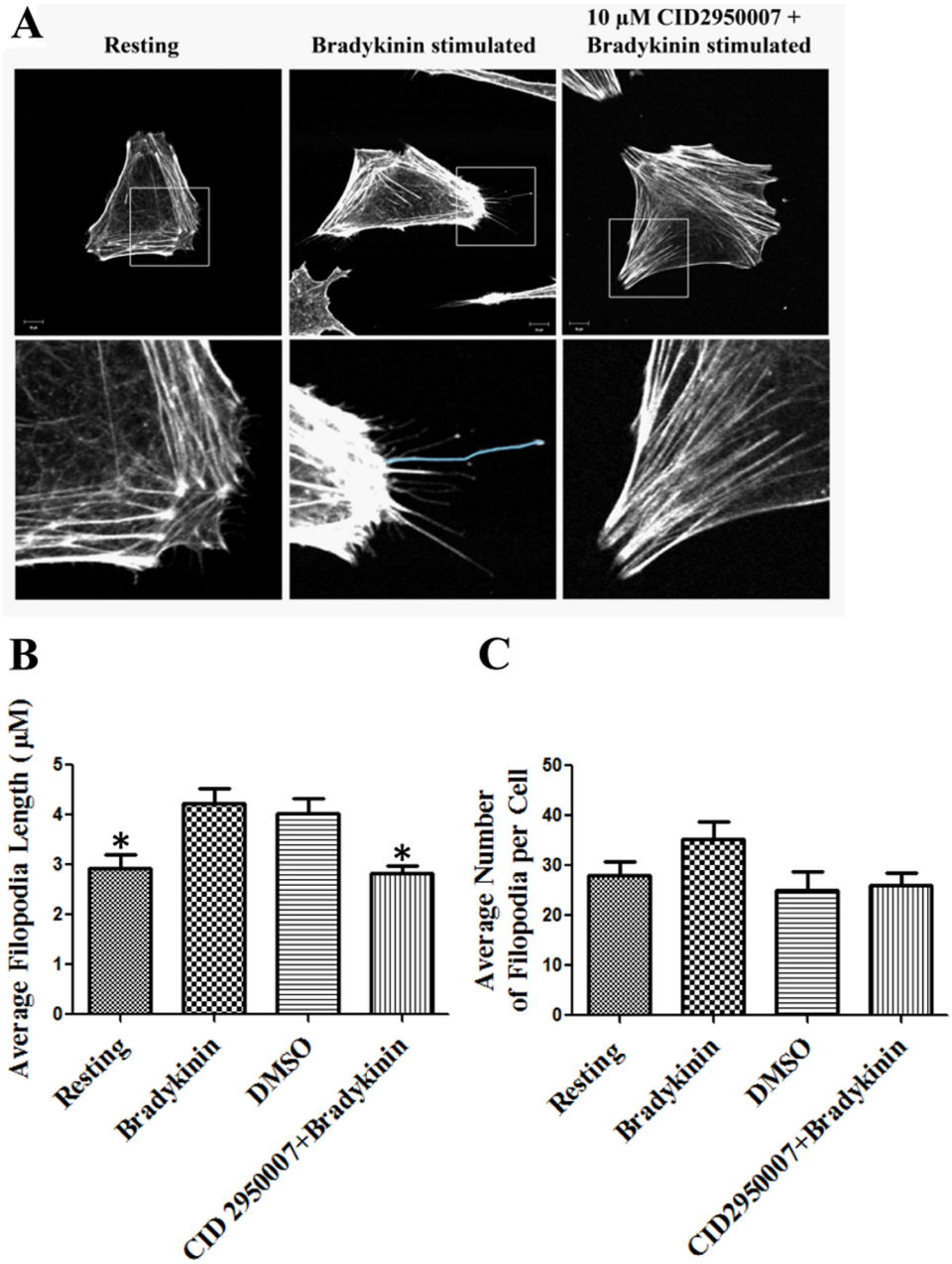


FIGURE 5. **CID2950007 decreased filopodia formation in 3T3 cells after bradykinin treatment.** *A*, representative images of resting control cells, cells stimulated with 100 ng/ml bradykinin, and cells incubated with 10 $\mu$M CID2950007 for 1 h before the addition of bradykinin. Cells were permeabilized and stained as described under "Experimental Procedures" before the pictures were taken on a Zeiss LSM 510 Meta. *Lower panels* show 6.5-fold magnified views of *boxed areas* in *top panels*. The *blue line* shows tracing of filopodia for quantification. *B*, numbers of filopodia per cell. *C*, length of filopodia on each cell, 1 $\mu$m = 28.5 pixels. The experiment was repeated three times, and 30–60 cells were randomly imaged and analyzed. Mean lengths or number of filopodia ± S.E. from a single experiment are plotted. *Asterisks* denote $p < 0.05$ based on one-way ANOVA with Dunnett's post test relative to bradykinin-stimulated control cells.

due to the effects of multiple intracellular regulators that facilitate the nucleotide association and hydrolysis. Because CID2950007 is a Cdc42-selective inhibitor, our observation suggests the involvement of Cdc42 in the integrin VLA-4 signaling pathway. In addition, this analysis also allowed a real-time evaluation of the rate at which CID2950007 entered the cells and exerted its inhibitory effect.

## DISCUSSION

The pursuit of GTPase inhibitors has been an enduring effort due to the important roles that this class of proteins plays in cell physiology and the strong indications they have in cancers, immune diseases, and neurological disorders (53–56). Specifically, Cdc42 has been implicated in ovarian cancer (16), breast cancer (57), hepatitis C virus-related liver disease (58), and mental retardation (59). However, there has been limited success in GTPase inhibitor discovery. Prior Cdc42 inhibitors either lack selectivity by acting on multiple GTPases or only target particular protein-protein interactions (19, 60). The function of Cdc42 is controlled by multiple upstream regulators and downstream effectors (41). Blocking one set of interactions may be useful in some sce-

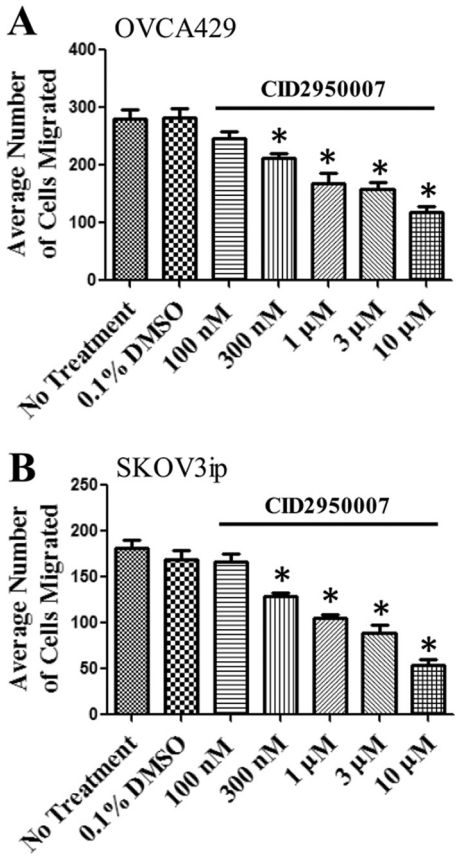


FIGURE 6. **CID2950007 inhibited the migration of OVCA429 (*A*) and SKOV3ip (*B*) cells in a dose-dependent manner.** Cells were allowed to attach to the Boyden chambers. CID2950007 at indicated concentrations were added to the growth media. Membrane filters were imaged 48 h later. All assays represent three independent trials with three representative fields counted for each treatment. Means ± S.E. from all trials are plotted. *Asterisks* denote $p < 0.05$ based on one-way ANOVA with Dunnett's post test and relative to migration of untreated control cells. Statistical significance was the same when treated samples were compared with 0.1% DMSO treatment group.

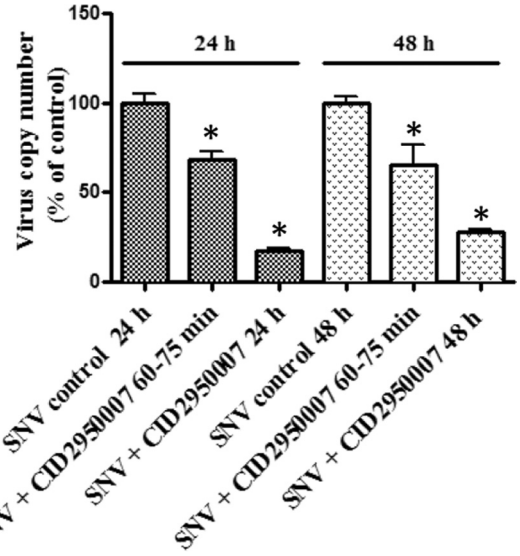


FIGURE 7. **CID2950007 inhibited Sin Nombre virus infection efficiency.** CID2950007 at 10 $\mu$M was added to host Vero E6 cells either only during virus contact (60–75 min) followed by reincubation for 24–48 h in the absence of the compound or during virus contact and maintained throughout the culturing period after viral contact (24–48 h). The two conditions provide an indication of CID2950007 effects on virus entry alone as compared with effects on virus entry and replication. Viral RNA content was quantified after 24 or 48 h as described under "Experimental Procedures." Viral infection experiments were repeated three times with 3–6 replicates per trial. Means ± S.E. from all trials are plotted. *Asterisks* denote $p < 0.05$ based on one-way ANOVA with Dunnett's post test and relative to infected control cells without compound treatment at the relevant time point. *SNV*, Sin Nombre virions.

narios. However, the protein could still remain active by interacting with other partners and allow undesirable bypasses. Moreover, sequestering a shared GDI would affect the function of other GTPases. We report here the characterization of a selective small molecule inhibitor for Cdc42 and a second active analog. Numerous other structurally related analogs were tested and found inactive (supplemental Fig. S1), confirming specificity. The compounds inhibit Cdc42 while sparing Rac and Rho that are in the same GTPase family and have high sequence and structure homology to Cdc42. Furthermore, using a real-time fluorescence assay, CID2950007 was shown to be an allosteric inhibitor that binds the guanine nucleotide-associated Cdc42 and induces ligand dissociation. Supplemental Fig. S2 shows predicted docking of the compounds. In collaboration with Dr. Roger Goody (Max-Planck Institute of Physical Chemistry, Dortmund, Germany), crystallization trials were conducted and led to the conclusion that the synthesis of derivatives that can be covalently cross-linked to the GTPase will be required. It also remains to be determined how the compound affects RhoV, RhoU, and RhoJ GTPases that are often expressed in a cell type-specific manner and are classified as Cdc42-like GTPases (61, 62).

BODIPY® FL GTP has been widely used in research with guanine nucleotide-binding proteins because of its high sensitivity and the minimal interference from the fluorescent label (63). As compared with radioisotope-labeled nucleotide analogs, it is environmentally friendly and convenient to use. The fact that CID2950007 was discovered in a fluorescence-based screening campaign using BODIPY® FL GTP (21) and in the present study validated in multiple biochemical and cellular assays again proved the effectiveness of BODIPY®-labeled guanine nucleotide in GTPase studies.

Many currently available GTPase inhibitors target protein-protein interaction interfaces. Dbs is a GEF for both Cdc42 and RhoA. Whether CID2950007 can affect Dbs-facilitated guanine nucleotide exchange on Cdc42 was tested with minimal effect detected (supplemental Fig. S3). Because the compound can displace both GDP and GTP and is inhibitory in cell-based assays, the compound could act independent of any effect on GEF activity or interaction, as supported by the docking studies (supplemental Fig. S2). In this model, consistent with the proposed allosteric mechanism, the compound is found to bind to an allosteric pocket adjacent to the nucleotide binding site to promote nucleotide dissociation and thus would not interfere with GEF binding to the switch regions (supplemental Fig. S2). However, small molecules may block a selective subset of protein-protein interactions as exemplified by NSC23766, which blocks Rac1 interaction with the Tiam and Trio GEFs, but not with Vav (64). There-

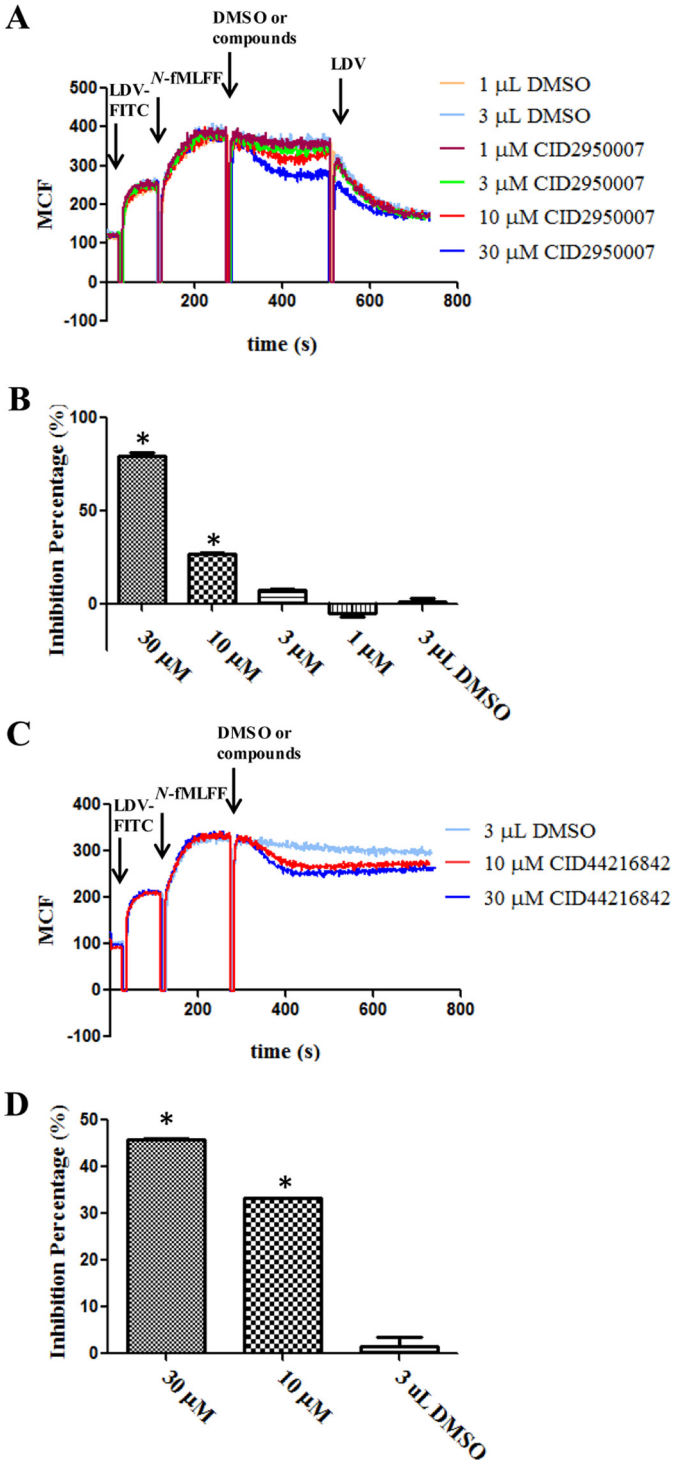


FIGURE 8. **CID2950007 inhibited VLA-4 activation in a dose-dependent manner.** *A*, VLA-4 activation status is monitored in real time. LDV-FITC was first added to U937 FPRΔST cells to achieve resting state binding ($K_d$ ~12 nM) (25). Then, *N*-formyl peptide (*N*-fMLFF) was added to stimulate VLA-4 activation. When the ligand binding reached equilibrium, CID2950007 at the indicated concentrations or an equal volume of DMSO was added. Nonfluorescent LDV was added to dissociate remaining LDV-FITC. *B*, quantification of the CID2950007 inhibition effects. The inhibition percentage was calculated according to supplemental Equation 3. At least three independent trials were performed with each trial in duplicate. *C*, representative curves from one trial are shown. *B* and *D*, means ± S.E. from one trial are plotted. *Asterisks* denote $p < 0.05$ based on one-way ANOVA with Dunnett's post test and relative to DMSO treatment.

fore, it is still too early to conclude whether CID2950007 could affect the interaction between Cdc42 and its other specific GEFs besides being able to block the guanine nucleotide binding to the GTPase.

Previously, the function of Cdc42 in mammalian cells has been studied using its dominant-negative or constitutively active mutants (65–67). However, these mutants can impede the functions of other GTPases with which Cdc42 shares upstream regulators and downstream effectors. For instance, a dominant-negative mutant can bind a shared GEF, whereas a constitutively active mutant may occupy a mutual effector, making them unavailable to other GTPases. Therefore, such an approach imposes limitations related to specificity, dosage, and clonal variability (68). The use of a small molecule-selective inhibitor instead achieves selective inactivation of Cdc42 within a short time window and leaves analogous GTPases unaffected. This should greatly facilitate the functional assignment of Cdc42 and help to disentangle complex GTPase networks.

Due to its important roles in cytoskeleton organization, the activity of Cdc42 could be assessed in filopodia formation and cell migration assays. We observed that CID2950007 effectively inhibited Cdc42 in both assays, leading to less filopodia formation and ineffective cell migration. Contrary to our observation that Cdc42 promoted chemotaxis, which was inhibited by CID2950007, some early studies reported that Cdc42 negatively regulated cell migration (69). This might be because the function of Cdc42 is cell type-specific (42), or is likely due to the use of constitutively active Cdc42 mutants in those studies that may induce nonspecific effects and bias the conclusions. This again shows the value of small molecule-selective inhibitors.

Rac and Rho have been shown to be involved in the inside-out signaling pathways triggered by chemokines. The signaling results in $\alpha4\beta1$-dependent up-regulation of the adhesion capacity of T-lymphocytes and leukocytes (50–52). The involvement of Cdc42 in the same GTPase family remains unknown. In this study, the use of the small molecule Cdc42-selective inhibitor strongly suggests the participation of Cdc42. The briefness of the decrease of the fluorescence level, which is an indication of the VLA-4 activation state, indicates that redundant signaling pathways are capable of compensating the inhibited Cdc42 (70). Moreover, our assay represents a breakthrough in the methodology to study the involvement of GTPases in integrin activation. Previous studies typically used either immunoprecipitation or radioactive labeling to isolate GTPases from the cell lysate and quantify nucleotide incorporation (50–52). Such efforts are often time-consuming and involve complicated waste disposal. In addition, they would not reveal the concurrent changes happening in the cells. On the other hand, our assay could conveniently monitor the adhesion changes of the cells in real time by using flow cytometry and fluorescently labeled peptide.

In conclusion, we characterized a small molecule allosteric inhibitor that selectively inhibits nucleotide binding to the Cdc42 GTPase. The compound may find its applications in drug development aimed at Cdc42-related diseases. As illus-

trated by the examples, the compound can also help to unravel the complex signaling pathways that often involve multiple GTPases.

*Acknowledgments—The raw data obtained from the CyAn™ ADP flow cytometer was parsed by the HyperView® software developed by Dr. Bruce Edward at the University of New Mexico. Images in this paper were generated in the University of New Mexico and Cancer Center Fluorescence Microscopy Shared Resource. We thank Matthew Garcia for technical assistance; Kristine Gouveia, Dr. Mark Haynes, and Dr. Peter Simons for critical reading of the manuscript; and Dr. Edward Bedrick for advice on statistical analyses. A.W.N., supported by a DAAD fellowship, conducted these studies in the laboratory of Dr. Roger Goody in October 2011.*

## REFERENCES


1. Bender, A., and Pringle, J. R. (1989) Multicopy suppression of the *cdc24* budding defect in yeast by *CDC42* and three newly identified genes including the *ras*-related gene *RSR1*. *Proc. Natl. Acad. Sci. U.S.A.* **86,** 9976–9980
2. Cotteret, S., and Chernoff, J. (2002) The evolutionary history of effectors downstream of Cdc42 and Rac. *Genome Biol.* **3,** REVIEWS0002
3. Bos, J. L., Rehmann, H., and Wittinghofer, A. (2007) GEFs and GAPs: critical elements in the control of small G proteins. *Cell* **129,** 865–877
4. Bishop, A. L., and Hall, A. (2000) Rho GTPases and their effector proteins. *Biochem. J.* **348,** 241–255
5. Ridley, A. J. (2006) Rho GTPases and actin dynamics in membrane protrusions and vesicle trafficking. *Trends Cell Biol.* **16,** 522–529
6. Stengel, K., and Zheng, Y. (2011) Cdc42 in oncogenic transformation, invasion, and tumorigenesis. *Cell. Signal.* **23,** 1415–1423
7. Harris, K. P., and Tepass, U. (2010) Cdc42 and vesicle trafficking in polarized cells. *Traffic* **11,** 1272–1279
8. Chimini, G., and Chavrier, P. (2000) Function of Rho family proteins in actin dynamics during phagocytosis and engulfment. *Nat. Cell Biol.* **2,** E191–E196
9. Kamai, T., Yamanishi, T., Shirataki, H., Takagi, K., Asami, H., Ito, Y., and Yoshida, K. (2004) Overexpression of RhoA, Rac1, and Cdc42 GTPases is associated with progression in testicular cancer. *Clin. Cancer Res.* **10,** 4799–4805
10. Chen, Q. Y., Jiao, D. M., Yao, Q. H., Yan, J., Song, J., Chen, F. Y., Lu, G. H., and Zhou, J. Y. (2012) Expression analysis of Cdc42 in lung cancer and modulation of its expression by curcumin in lung cancer cell lines. *Int. J. Oncol.* **40,** 1561–1568
11. Asnaghi, L., Vass, W. C., Quadri, R., Day, P. M., Qian, X., Braverman, R., Papageorge, A. G., and Lowy, D. R. (2010) E-cadherin negatively regulates neoplastic growth in non-small cell lung cancer: role of Rho GTPases. *Oncogene* **29,** 2760–2771
12. Tucci, M. G., Lucarini, G., Brancorsini, D., Zizzi, A., Pugnaloni, A., Giacchetti, A., Ricotti, G., and Biagini, G. (2007) Involvement of E-cadherin, β-catenin, Cdc42, and CXCR4 in the progression and prognosis of cutaneous melanoma. *Br. J. Dermatol.* **157,** 1212–1216
13. Nalla, A. K., Asuthkar, S., Bhoopathi, P., Gujrati, M., Dinh, D. H., and Rao, J. S. (2010) Suppression of uPAR retards radiation-induced invasion and migration mediated by integrin β1/FAK signaling in medulloblastoma. *PloS one* **5,** e13006
14. Ahn, S. J., Chung, K. W., Lee, R. A., Park, I. A., Lee, S. H., Park, D. E., and Noh, D. Y. (2003) Overexpression of βPix-a in human breast cancer tissues. *Cancer Lett.* **193,** 99–107
15. Cheung, L. W., Leung, P. C., and Wong, A. S. (2010) Cadherin switching and activation of p120 catenin signaling are mediators of gonadotropin-releasing hormone to promote tumor cell migration and invasion in ovarian cancer. *Oncogene* **29,** 2427–2440
16. Ip, C. K., Cheung, A. N., Ngan, H. Y., and Wong, A. S. (2011) p70 S6 kinase in the control of actin cytoskeleton dynamics and directed migration of ovarian cancer cells. *Oncogene* **30,** 2420–2432
17. Pandey, R. N., Rani, R., Yeo, E. J., Spencer, M., Hu, S., Lang, R. A., and Hegde, R. S. (2010) The Eyes Absent phosphatase-transactivator proteins promote proliferation, transformation, migration, and invasion of tumor cells. *Oncogene* **29,** 3715–3722
18. Sehr, P., Joseph, G., Genth, H., Just, I., Pick, E., and Aktories, K. (1998) Glucosylation and ADP ribosylation of Rho proteins: effects on nucleotide binding, GTPase activity, and effector coupling. *Biochemistry* **37,** 5296–5304
19. Pelish, H. E., Peterson, J. R., Salvarezza, S. B., Rodriguez-Boulan, E., Chen, J. L., Stamnes, M., Macia, E., Feng, Y., Shair, M. D., and Kirchhausen, T. (2006) Secramine inhibits Cdc42-dependent functions in cells and Cdc42 activation *in vitro*. *Nat. Chem. Biol.* **2,** 39–46
20. Kohl, N. E., Mosser, S. D., deSolms, S. J., Giuliani, E. A., Pompliano, D. L., Graham, S. L., Smith, R. L., Scolnick, E. M., Oliff, A., and Gibbs, J. B. (1993) Selective inhibition of Ras-dependent transformation by a farnesyltransferase inhibitor. *Science* **260,** 1934–1937
21. Surviladze, Z., Waller, A., Strouse, J. J., Bologa, C., Ursu, O., Salas, V., Parkinson, J. F., Phillips, G. K., Romero, E., Wandinger-Ness, A., Sklar, L. A., Schroeder, C., Simpson, D., Noth, J., Wang, J., Golden, J., and Aube, J. (2010) A Potent and Selective Inhibitor of Cdc42 GTPase. in *Probe Reports from the NIH Molecular Libraries Program*, National Institutes of Health, Bethesda, MD
22. Surviladze, Z., Waller, A., Wu, Y., Romero, E., Edwards, B. S., Wandinger-Ness, A., and Sklar, L. A. (2010) Identification of a small GTPase inhibitor using a high-throughput flow cytometry bead-based multiplex assay. *J. Biomol. Screen.* **15,** 10–20
23. Surviladze, Z., Young, S. M., and Sklar, L. A. (2012) High-throughput flow cytometry bead-based multiplex assay for identification of Rho GTPase inhibitors. *Methods Mol. Biol.* **827,** 253–270
24. Schwartz, S. L., Tessema, M., Buranda, T., Pylypenko, O., Rak, A., Simons, P. C., Surviladze, Z., Sklar, L. A., and Wandinger-Ness, A. (2008) Flow cytometry for real-time measurement of guanine nucleotide binding and exchange by Ras-like GTPases. *Anal. Biochem.* **381,** 258–266
25. Chigaev, A., Blenc, A. M., Braaten, J. V., Kumaraswamy, N., Kepley, C. L., Andrews, R. P., Oliver, J. M., Edwards, B. S., Prossnitz, E. R., Larson, R. S., and Sklar, L. A. (2001) Real time analysis of the affinity regulation of α4-integrin. The physiologically activated receptor is intermediate in affinity between resting and $Mn^{2+}$ or antibody activation. *J. Biol. Chem.* **276,** 48670–48678
26. Tsao, S. W., Mok, S. C., Fey, E. G., Fletcher, J. A., Wan, T. S., Chew, E. C., Muto, M. G., Knapp, R. C., and Berkowitz, R. S. (1995) Characterization of human ovarian surface epithelial cells immortalized by human papilloma viral oncogenes (HPV-E6E7 ORFs). *Exp. Cell Res.* **218,** 499–507
27. Reeder, M. K., Serebriiskii, I. G., Golemis, E. A., and Chernoff, J. (2001) Analysis of small GTPase signaling pathways using p21-activated kinase mutants that selectively couple to Cdc42. *J. Biol. Chem.* **276,** 40606–40613
28. Reid, T., Furuyashiki, T., Ishizaki, T., Watanabe, G., Watanabe, N., Fujisawa, K., Morii, N., Madaule, P., and Narumiya, S. (1996) Rhotekin, a new putative target for Rho bearing homology to a serine/threonine kinase, PKN, and rhophilin in the Rho-binding domain. *J. Biol. Chem.* **271,** 13556–13560
29. Kozma, R., Ahmed, S., Best, A., and Lim, L. (1995) The Ras-related protein Cdc42Hs and bradykinin promote formation of peripheral actin microspikes and filopodia in Swiss 3T3 fibroblasts. *Mol. Cell. Biol.* **15,** 1942–1952
30. Botten, J., Mirowsky, K., Kusewitt, D., Ye, C., Gottlieb, K., Prescott, J., and Hjelle, B. (2003) Persistent Sin Nombre virus infection in the deer mouse (*Peromyscus maniculatus*) model: sites of replication and strand-specific expression. *J. Virol.* **77,** 1540–1550
31. Prescott, J. B., Hall, P. R., Bondu-Hawkins, V. S., Ye, C., and Hjelle, B. (2007) Early innate immune responses to Sin Nombre hantavirus occur independently of IFN regulatory factor 3, characterized pattern recognition receptors, and viral entry. *J. Immunol.* **179,** 1796–1802
32. Chigaev, A., and Sklar, L. A. (2012) Overview: assays for studying integrin-dependent cell adhesion. *Methods Mol. Biol.* **757,** 3–14
33. Potter, R. M., Maestas, D. C., Cimino, D. F., and Prossnitz, E. R. (2006) Regulation of *N*-formyl peptide receptor signaling and trafficking by individual carboxyl-terminal serine and threonine residues. *J. Immunol.* **176,**

5418–5425
34. Copeland, R. A. (2005) *Evaluation of Enzyme Inhibitors in Drug Discovery: A Guide for Medicinal Chemists and Pharmacologists*, Wiley-Interscience, Hoboken, NJ
35. Torimura, M., Kurata, S., Yamada, K., Yokomaku, T., Kamagata, Y., Kanagawa, T., and Kurane, R. (2001) Fluorescence-quenching phenomenon by photoinduced electron transfer between a fluorescent dye and a nucleotide base. *Anal. Sci.* **17,** 155–160
36. Korlach, J., Baird, D. W., Heikal, A. A., Gee, K. R., Hoffman, G. R., and Webb, W. W. (2004) Spontaneous nucleotide exchange in low molecular weight GTPases by fluorescently labeled γ-phosphate-linked GTP analogs. *Proc. Natl. Acad. Sci. U.S.A.* **101,** 2800–2805
37. Zhang, B., Zhang, Y., Wang, Z., and Zheng, Y. (2000) The role of $Mg^{2+}$ cofactor in the guanine nucleotide exchange and GTP hydrolysis reactions of Rho family GTP-binding proteins. *J. Biol. Chem.* **275,** 25299–25307
38. Nobes, C. D., and Hall, A. (1995) Rho, Rac, and cdc42 GTPases regulate the assembly of multimolecular focal complexes associated with actin stress fibers, lamellipodia, and filopodia. *Cell* **81,** 53–62
39. Ashman, L. K., and Gesche, A. H. (1985) Surface antigen expression by a human B-lymphoblastoid cell line treated with 'differentiation' inducers, dimethysulfoxide and tetradecanoylphorbol acetate. *Leuk. Res.* **9,** 157–165
40. Yumura, S., and Fukui, Y. (1983) Filopodelike projections induced with dimethyl sulfoxide and their relevance to cellular polarity in *Dictyostelium*. *J. Cell Biol.* **96,** 857–865
41. Etienne-Manneville, S., and Hall, A. (2002) Rho GTPases in cell biology. *Nature* **420,** 629–635
42. Yang, L., Wang, L., and Zheng, Y. (2006) Gene targeting of Cdc42 and Cdc42GAP affirms the critical involvement of Cdc42 in filopodia induction, directed migration, and proliferation in primary mouse embryonic fibroblasts. *Mol. Biol. Cell* **17,** 4675–4685
43. Etienne-Manneville, S., and Hall, A. (2003) Cdc42 regulates GSK-3β and adenomatous polyposis coli to control cell polarity. *Nature* **421,** 753–756
44. Bourguignon, L. Y., Gilad, E., Rothman, K., and Peyrollier, K. (2005) Hyaluronan-CD44 interaction with IQGAP1 promotes Cdc42 and ERK signaling, leading to actin binding, Elk-1/estrogen receptor transcriptional activation, and ovarian cancer progression. *J. Biol. Chem.* **280,** 11961–11972
45. Mythreye, K., and Blobe, G. C. (2009) The type III TGF-β receptor regulates epithelial and cancer cell migration through β-arrestin2-mediated activation of Cdc42. *Proc. Natl. Acad. Sci. U.S.A.* **106,** 8221–8226
46. Mercer, J., and Helenius, A. (2009) Virus entry by macropinocytosis. *Nat. Cell Biol.* **11,** 510–520
47. Naranatt, P. P., Krishnan, H. H., Smith, M. S., and Chandran, B. (2005) Kaposi's sarcoma-associated herpesvirus modulates microtubule dynamics via RhoA-GTP-diaphanous 2 signaling and utilizes the dynein motors to deliver its DNA to the nucleus. *J. Virol.* **79,** 1191–1206
48. Petermann, P., Haase, I., and Knebel-Mörsdorf, D. (2009) Impact of Rac1 and Cdc42 signaling during early herpes simplex virus type 1 infection of keratinocytes. *J. Virol.* **83,** 9759–9772
49. Nikolic, D. S., Lehmann, M., Felts, R., Garcia, E., Blanchet, F. P., Subramaniam, S., and Piguet, V. (2011) HIV-1 activates Cdc42 and induces membrane extensions in immature dendritic cells to facilitate cell-to-cell virus propagation. *Blood* **118,** 4841–4852
50. García-Bernal, D., Wright, N., Sotillo-Mallo, E., Nombela-Arrieta, C., Stein, J. V., Bustelo, X. R., and Teixidó, J. (2005) Vav1 and Rac control chemokine-promoted T lymphocyte adhesion mediated by the integrin α4β1. *Mol. Biol. Cell* **16,** 3223–3235
51. Laudanna, C., Campbell, J. J., and Butcher, E. C. (1996) Role of Rho in chemoattractant-activated leukocyte adhesion through integrins. *Science* **271,** 981–983
52. Woodside, D. G., Wooten, D. K., Teague, T. K., Miyamoto, Y. J., Caudell, E. G., Udagawa, T., Andruss, B. F., and McIntyre, B. W. (2003) Control of T lymphocyte morphology by the GTPase Rho. *BMC Cell Biol.* **4,** 2
53. Antoine-Bertrand, J., Villemure, J. F., and Lamarche-Vane, N. (2011) Implication of Rho GTPases in neurodegenerative diseases. *Curr. Drug Targets* **12,** 1202–1215
54. Mitra, S., Cheng, K. W., and Mills, G. B. (2011) Rab GTPases implicated in inherited and acquired disorders. *Semin. Cell Dev. Biol.* **22,** 57–68
55. Shaw, R. J., and Cantley, L. C. (2006) Ras, PI(3)K and mTOR signalling controls tumour cell growth. *Nature* **441,** 424–430
56. Rathinam, R., Berrier, A., and Alahari, S. K. (2011) Role of Rho GTPases and their regulators in cancer progression. *Front. Biosci.* **16,** 2561–2571
57. Kikuchi, K., Li, X., Zheng, Y., and Takano, Y. (2011) Invasion of breast cancer cells into collagen matrix requires TGF-α and Cdc42 signaling. *FEBS Lett.* **585,** 286–290
58. Smith, M. W., Yue, Z. N., Korth, M. J., Do, H. A., Boix, L., Fausto, N., Bruix, J., Carithers, R. L., Jr., and Katze, M. G. (2003) Hepatitis C virus and liver disease: global transcriptional profiling and identification of potential markers. *Hepatology* **38,** 1458–1467
59. Kreis, P., Thévenot, E., Rousseau, V., Boda, B., Muller, D., and Barnier, J. V. (2007) The p21-activated kinase 3 implicated in mental retardation regulates spine morphogenesis through a Cdc42-dependent pathway. *J. Biol. Chem.* **282,** 21497–21506
60. Just, I., Selzer, J., Hofmann, F., Green, G. A., and Aktories, K. (1996) Inactivation of Ras by *Clostridium sordellii* lethal toxin-catalyzed glucosylation. *J. Biol. Chem.* **271,** 10149–10153
61. Faure, S., and Fort, P. (2011) Atypical RhoV and RhoU GTPases control development of the neural crest. *Small GTPases* **2,** 310–313
62. Leszczynska, K., Kaur, S., Wilson, E., Bicknell, R., and Heath, V. L. (2011) The role of RhoJ in endothelial cell biology and angiogenesis. *Biochem. Soc. Trans.* **39,** 1606–1611
63. McEwen, D. P., Gee, K. R., Kang, H. C., and Neubig, R. R. (2001) Fluorescent BODIPY-GTP analogs: real-time measurement of nucleotide binding to G proteins. *Anal. Biochem.* **291,** 109–117
64. Gao, Y., Dickerson, J. B., Guo, F., Zheng, J., and Zheng, Y. (2004) Rational design and characterization of a Rac GTPase-specific small molecule inhibitor. *Proc. Natl. Acad. Sci. U.S.A.* **101,** 7618–7623
65. Hall, A. (1998) Rho GTPases and the actin cytoskeleton. *Science* **279,** 509–514
66. Johnson, D. I. (1999) Cdc42: An essential Rho-type GTPase controlling eukaryotic cell polarity. *Microbiol. Mol. Biol. Rev.* **63,** 54–105
67. Lamarche, N., Tapon, N., Stowers, L., Burbelo, P. D., Aspenström, P., Bridges, T., Chant, J., and Hall, A. (1996) Rac and Cdc42 induce actin polymerization and G1 cell cycle progression independently of p65PAK and the JNK/SAPK MAP kinase cascade. *Cell* **87,** 519–529
68. Melendez, J., Grogg, M., and Zheng, Y. (2011) Signaling role of Cdc42 in regulating mammalian physiology. *J. Biol. Chem.* **286,** 2375–2381
69. Shimonaka, M., Katagiri, K., Nakayama, T., Fujita, N., Tsuruo, T., Yoshie, O., and Kinashi, T. (2003) Rap1 translates chemokine signals to integrin activation, cell polarization, and motility across vascular endothelium under flow. *J. Cell Biol.* **161,** 417–427
70. Giagulli, C., Scarpini, E., Ottoboni, L., Narumiya, S., Butcher, E. C., Constantin, G., and Laudanna, C. (2004) RhoA and ζ PKC control distinct modalities of LFA-1 activation by chemokines: critical role of LFA-1 affinity triggering in lymphocyte *in vivo* homing. *Immunity* **20,** 25–35